SUPPORTING INFORMATION SECTION

# Oxidation of Benzene by Fe(III)- and Mn(IV)-Containing Oxides: Stoichiometric Efficiency and Transformation Products

Haizhou Liu[†], Thomas A. Bruton[‡], Wei Li[†], Jean Van Buren‡, Carsten Prasse[‡], Fiona M. Doyle[§], and David L. Sedlak*[‡]

[†] Department of Chemical and Environmental Engineering, University of California at Riverside, Riverside, CA 92521 USA

[‡] Department of Civil and Environmental Engineering, University of California at Berkeley, Berkeley, CA 94720 USA

[§] Department of Material Science and Engineering, University of California at Berkeley, Berkeley, CA 94720 USA

*Submitted to Environmental Science & Technology*

* Corresponding author, e-mail: sedlak@berkeley.edu, phone (510) 643-0256

# Table of Content

**Text S1: Experimental setup and material preparation**

All chemicals used in this study were reagent grade or higher. Solutions were prepared using deionized water (resistivity >18.2 MΩ, Millipore system). Four types of pure minerals were employed in this study, *i.e.*, amorphous ferrihydrite ($Fe(OH)_{3(s)}$), goethite ($\alpha$-$FeOOH_{(s)}$), pyrolusite ($\beta$-$MnO_{2(s)}$) and silica ($SiO_2$). Pyrolusite and ferrihydrite were directly obtained from Sigma-Aldrich. Pyrolusite was used without further processing. Ferrihydrite was aged in deionized water buffered at pH 8.0 with 50 mM borate for 2 weeks prior to experiments, with daily pH adjustment to 8.0 by adding 1 mM NaOH. After that, ferrihydrite suspension was centrifuged and the particles were washed three times with deionized water before finally dried with a freeze dry system. Silica obtained as pure sand (ACROS Organics) was rinsed in 0.1 M $HClO_4$ at a concentration of 300 g/L. After 24 hours, the solution was decanted and replaced. This step was repeated for 3 consecutive days. After that, silica particles were freeze-dried. Goethite was synthesized by aging freshly made ferrihydrite in a concentrated NaOH solution at 70 ºC for 60 hours. Two clay materials, nontronite and montmorillonite were used. Five aquifer solids were used, denoted as AWBPH, AFTCS, CAROL, CADOU and AMTAL. The characterization of materials is listed in Table S1 and can be found in a recently published paper.[1].

**Text S2: Control of dissolved $O_2$ concentration in samples**

The dissolved $O_2$ concentration in the solution was adjusted by purging with air, $N_2$, or pure $O_2$. In most cases, the solution was saturated with air (*i.e.*, with a dissolved $O_2$ concentration of 250 μM). In cases where $O_2$-free conditions were needed, the suspension was purged with $N_2$ and kept in a glove box during the experiments. For those samples, the residual $O_2$ concentration was always less than 3 μM. For experiments conducted at elevated $O_2$ concentrations, the solution was purged with pure $O_2$ in a 1-L volumetric flask without headspace at 4°C and was sealed before raising the temperature back to 23°C. This process yielded a dissolved $O_2$ concentration of 410 μM.

**Text S3: High-resolution mass spectrometry and its operating conditions**

Chromatographic separation was achieved using a Hydro-RP column (150 x 4.6 mm) equipped with a guard column (both Phenomenex). 0.1% Acetic acid (A) and methanol (B) were used as eluents. The percentage of (A) was changed linearly as follows: 0-2 min, 100%; 8 min, 40%; 11 min, 5%; 12 min, 5%, 12.1 min 100%, 18 min, 100%. Injection volume was set to 50 μL. QTOF analysis was performed in negative ESI-MS mode in both fullscan (80 – 400 m/z) and targeted MS/MS mode to obtain exact mass and structural information of the unknown compound. The source parameters were set to: gas temperature 300°C, gas flow: 12 L $min^{-1}$, nebulizer: 30 psi, capillary voltage: 3000 V.

**Text S4: Nuclear magnetic resonance (NMR) and solid-phase extraction (SPE)**

To prepare the sample for nuclear magnetic resonance (NMR), solid-phase extraction (SPE) was used to both separate the unknown compound from benzene and phenol and to concentrate the product. SPE cartridges (BondElut C18; 1g sorbent) were conditioned using 5 mL of heptane, 5 mL acetone and 5 mL methanol followed by 25 mL of DI water adjusted to pH 2 using 1 M $H_2SO_4$. To produce the unknown, 2 L of a 1mM benzene solution containing 10 mM persulfate were exposed to UV light from a low-pressure Hg lamp. Formation of the unknown compound was monitored by HPLC/UV and the experiments were terminated when its peak area reached a plateau (usually within 5 hours). Unbuffered ultrapure water was used to minimize potential interferences of salts in the NMR analysis. No significant differences between buffered and unbuffered water were observed with respect to the unknown compound. After loading the samples to SPE cartridges (50 mL per cartridge, sample pH was adjusted to pH 2), cartridges were first washed with 5 mL of DI water at pH 2. The unknown compound was then eluted using 10 mL of DI water at pH 7, leaving benzene and phenol on the cartridges for later elution with 10 mL of methanol. This procedure was repeated several times to achieve an overall enrichment factor of 200. The final sample was subjected once more to the SPE procedure described above but using $D_2O$ (pH 2) for washing of the cartridge and $CH_3CN$-$d_3$ for elution of the unknown. NMR analysis ($^1$H-NMR, $^1$H,$^1$H-COSY, $^1$H,$^1$H-NOESY, $^1$H,$^{13}$C-HSQC) was performed within 24 h to minimize degradation of the unknown compound. NMR spectra were acquired on a Bruker Avance 600 MHz instrument.

**Text S5: Proposed mechanism on the transformation of $S_2O_8^{\bullet-}$**

Previous kinetics studies did not specifically examine the decomposition pathways of persulfate radical ($S_2O_8^{\bullet-}$). If $S_2O_8^{\bullet-}$ were to react with metals to generate peroxymonosulfate $HSO_5^-$:

$$\equiv M^{n+} + S_2O_8^{\bullet-} + 2OH^- \rightarrow \equiv M^{(n-1)+} + 2HSO_5^- \quad \text{(S9)}$$

$HSO_5^-$ could reduce another metal, producing $SO_4^{\bullet-}$ and $O_2$:[9,2-4]

$$\equiv M^{n+} + HSO_5^- \rightarrow \equiv M^{(n-1)+} + SO_5^{\bullet-} + H^+ \quad \text{(S10)}$$

$$2SO_5^{\bullet-} \rightarrow 2SO_4^{\bullet-} + O_2 \quad \text{(S11)}$$

A combination of Reactions S9-S11 becomes:

$$3 \equiv M^{n+} + S_2O_8^{\bullet-} + 2OH^- \rightarrow 3 \equiv M^{(n-1)+} + 2SO_4^{\bullet-} + O_2 + 2H^+ \quad \text{(S12)}$$

Considering Reactions S1, S2 and S12, every 2 moles of $S_2O_8^{2-}$ generate 3 moles of $SO_4^{\bullet-}$, resulting in a maximum sulfate radical yeld of 150%. Alternatively, $S_2O_8^{\bullet-}$ could undergo reactions that do not produce additional sulfate radical, in which case the maximum sulfate radical yield for the overall process would be 50%.

Therefore, the decomposition of $S_2O_8^{\bullet-}$ through this mechanism could proceed through the pathway indicated below.

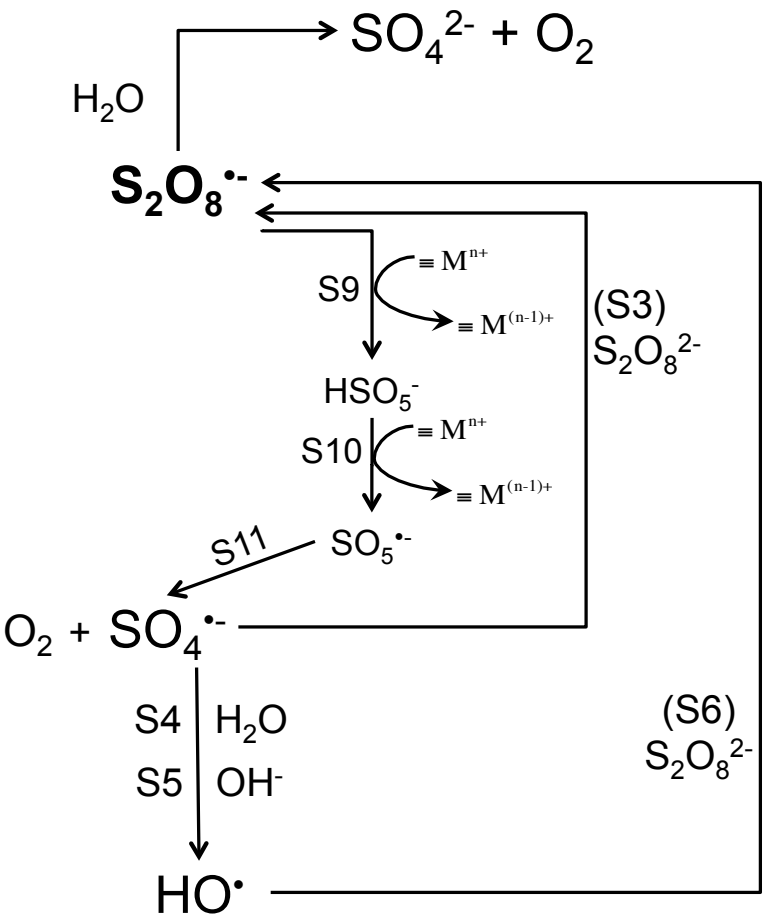
SO4 2- + O2
H2O
S2O8•-
≡ Mn+
S9
≡ M(n-1)+
(S3)
S2O8 2-
HSO5-
≡ Mn+
S10
≡ M(n-1)+
S11
SO5•-
O2 + SO4•-
S4
H2O
S5
OH-
(S6)
S2O8 2-
HO•

**Text S6: Kinetics of $SO_4^{\bullet-}$ and persulfate radical calculation**

*Fate of $SO_4^{\bullet-}$ in the absence of benzene:*

$SO_4^{\bullet-}$ is generated from Fenton-like reactions:

$$\equiv M^{n+} + S_2O_8^{2-} \rightarrow \equiv M^{(n-1)+} + S_2O_8^{\bullet-} \quad \text{(S1)}$$

$$\equiv M^{(n-1)+} + S_2O_8^{2-} \rightarrow \equiv M^{n+} + SO_4^{\bullet-} + SO_4^{2-} \quad \text{(S2)}$$

In the absence of benzene, there are three reactions that act as sinks for $SO_4^{\bullet-}$:[5,6,7]

$$SO_4^{\bullet-} + S_2O_8^{2-} \rightarrow S_2O_8^{\bullet-} + SO_4^{2-} \qquad k_3=6.3\times10^5\ M^{-1}s^{-1} \quad \text{(S3)}$$

$$SO_4^{\bullet-} + H_2O \rightarrow SO_4^{2-} + HO^{\bullet} + H^+ \qquad k_4=660\ s^{-1} \quad \text{(S4)}$$

$$SO_4^{\bullet-} + OH^- \rightarrow SO_4^{2-} + HO^{\bullet} \qquad k_5=7\times10^7\ M^{-1}s^{-1} \quad \text{(S5)}$$

When $S_2O_8^{2-}$ is activated (Reaction S1 to S2), one mole of $S_2O_8^{\bullet-}$ is generated for every mole of $SO_4^{\bullet-}$ generated. In addition, $S_2O_8^{2-}$ is also lost through reactions with $SO_4^{\bullet-}$ (Reaction S3). The branching ratio for $SO_4^{\bullet-}$ in the absence of benzene is $k_3[S_2O_8^{2-}]/(k_4 + k_5[OH^-])$. At pH 8 and 1 mM $S_2O_8^{2-}$, approximately half of the $SO_4^{\bullet-}$ reacts with $S_2O_8^{2-}$.

*Relative concentration of $SO_4^{\bullet-}$:*

In the absence of benzene, the major reaction that acts as a sink for $HO^{\bullet}$ is:[8,9]

$$HO^{\bullet} + S_2O_8^{2-} \rightarrow S_2O_8^{\bullet-} + OH^- \qquad k_6=1.4\times10^7\ M^{-1}s^{-1} \quad \text{(S6)}$$

$$\frac{d[HO^{\bullet}]}{dt} = k_4[SO_4^{\bullet-}] + k_5[OH^-][SO_4^{\bullet-}] - k_6[S_2O_8^{2-}][HO^{\bullet}]$$

Under steady-state conditions: $[HO^{\bullet}]_{ss} = \frac{k_4 + k_5[OH^-]}{k_6[S_2O_8^{2-}]}[SO_4^{\bullet-}]_{ss}$

With 1 mM $S_2O_8^{2-}$ and at pH 8.0, $[HO^{\bullet}]_{ss}=0.05[SO_4^{\bullet-}]_{ss}$. Therefore, the state-steady concentration of $SO_4^{\bullet-}$ is approximately 20 times higher than $HO^{\bullet}$ under experimental conditions employed in this study.

*Fate of $SO_4^{\bullet-}$ in the presence of benzene:*

In the presence of 1 mM benzene, the following reaction becomes the major sink for $SO_4^{\bullet-}$:

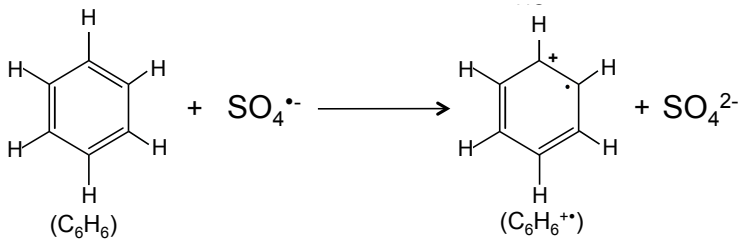


$k_7=3.0\times10^9\ M^{-1}s^{-1}$ (S7)

The branching ratio for $SO_4^{\bullet-}$ in the presence of benzene is $k_7$[benzene]/($k_3[S_2O_8^{2-}]+k_4+k_5[OH^-]$). At pH 8, 1 mM $S_2O_8^{2-}$ and 1 mM benzene, essentially all $SO_4^{\bullet-}$ reacts with benzene.

In the presence of benzene, there is an additional sink for $HO^{\bullet}$:[10]

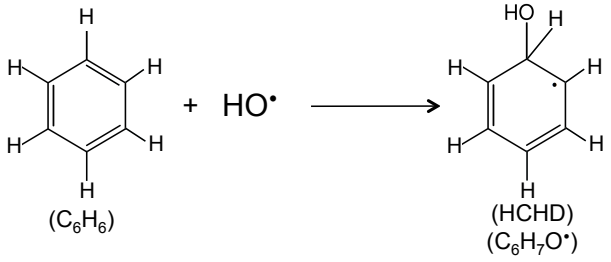


$k_8=7.9\times10^9\ M^{-1}s^{-1}$ (S8)

At steady-state conditions: $[HO^{\bullet}]_{ss}=\dfrac{k_4+k_5[OH^-]}{k_6[S_2O_8^{2-}]+k_8[benzene]}[SO_4^{\bullet-}]_{ss}$

With 1 mM benzene, 1 mM $S_2O_8^{2-}$ and at pH 8.0, $[HO^{\bullet}]_{ss}=0.01[SO_4^{\bullet-}]_{ss}$. Therefore, the state-steady concentration of $SO_4^{\bullet-}$ is still 2 orders of magnitude higher than $HO^{\bullet}$ under experimental conditions in the presence of benzene in this study.

**Text S7: Kinetics of organic radicals in the benzene/$SO_4^{\bullet-}$ system**

The hydroxylcyclohexadienyl (HCHD, *i.e.*, $C_6H_7O^{\bullet}$) radical can react with $O_2$ at the ortho position:[10]

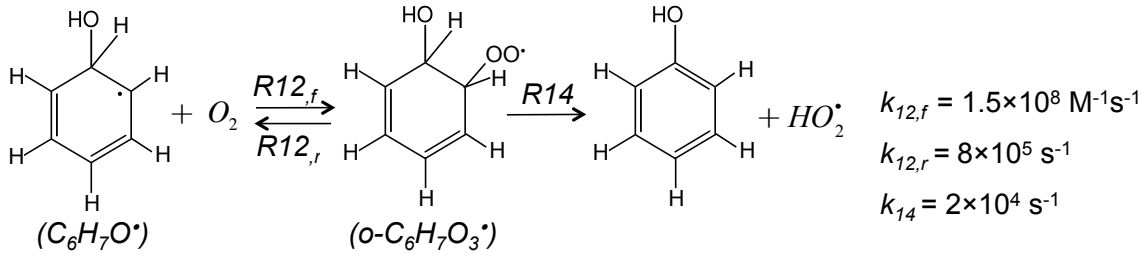


In addition, HCHD radical can react with $O_2$ at the *para*-position as follows:

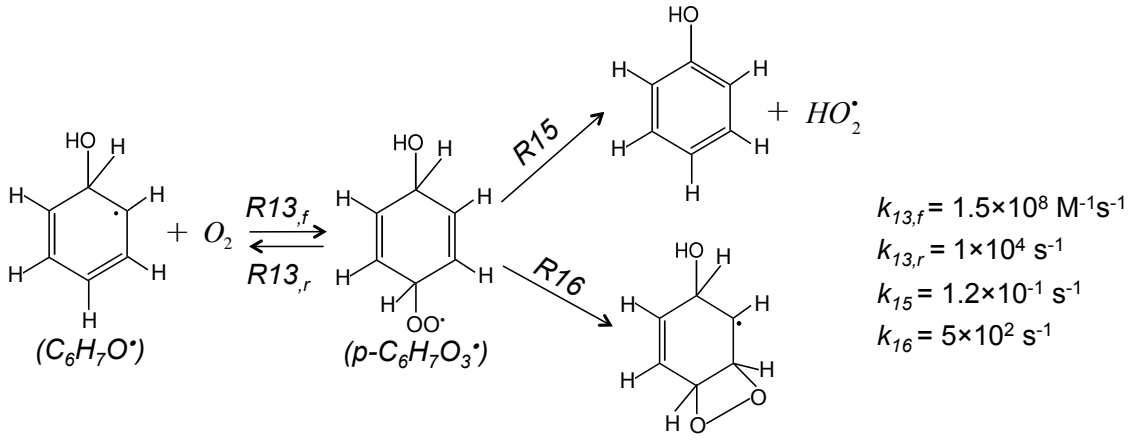


Based on the kinetics rate constants in Reactions 1 and 2,[10] the steady-state concentration of organic peroxy radicals are:

$$\frac{d[o\text{-}C_6H_7O_3^{\bullet}]}{dt} = k_{12,f}[O_2][HCHD] - k_{12,r}[o\text{-}C_6H_7O_3^{\bullet}] - k_{14}[o\text{-}C_6H_7O_3^{\bullet}] = 0$$

$$\frac{d[p\text{-}C_6H_7O_3^{\bullet}]}{dt} = k_{13,f}[O_2][HCHD] - k_{13,r}[p\text{-}C_6H_7O_3^{\bullet}] - k_{15}[p\text{-}C_6H_7O_3^{\bullet}] - k_{16}[p\text{-}C_6H_7O_3^{\bullet}] = 0$$

Under air-saturated conditions (*i.e.*, $[O_2]$=250 μM), the steady-state radical concentrations are:

$$[o\text{-}C_6H_7O_3^{\bullet}]_{ss} = \frac{k_1[O_2]}{k_{-1} + k_{1,f}}[HCHD]_{ss} = 0.045[HCHD]_{ss}$$

$$[p\text{-}C_6H_7O_3^{\bullet}]_{ss} = \frac{k_2[O_2]}{k_{-2} + k_{2,f} + k_{3,f}}[HCHD]_{ss} = 3.51[HCHD]_{ss}$$

Therefore: $[p\text{-}C_6H_7O_3^{\bullet}]_{ss} = 80[o\text{-}C_6H_7O_3^{\bullet}]_{ss}$ , and *p*-$C_6H_7O_3^{\bullet}$ accounts for 99% of $C_6H_7O_3^{\bullet}$.

The formation of phenol originates from both *o*-$C_6H_7O_3^{\bullet}$ and *p*-$C_6H_7O_3^{\bullet}$.

Because the branching ratio of $\frac{k_{1,f}[o\text{-}C_6H_7O_3^{\bullet}]_{ss}}{k_{2,f}[p\text{-}C_6H_7O_3^{\bullet}]_{ss}} = \frac{2\times10^4 \times 0.045[HCHD]_{ss}}{1.2\times10^{-1} \times 3.51[HCHD]_{ss}} = 2.1\times10^3$

Phenol is predominantly formed from *o*-$C_6H_7O_3^{\bullet}$.

**Text S8: Estimate of phenol loss due to direct reaction of $SO_4^{\bullet-}$ or $HO^{\bullet}$ with phenol in the presence of benzene.**

Phenol is produced from benzene reacting with $SO_4^{\bullet-}$:

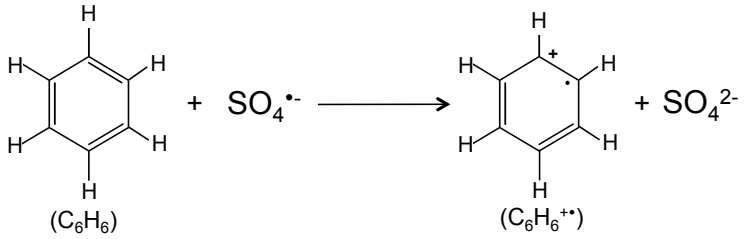


$k_7$=3.0×10$^9$ M$^{-1}$s$^{-1}$ (S7)

Phenol produced in this reaction can also react with $SO_4^{\bullet-}$:

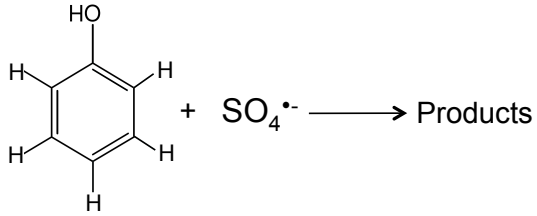


$k_{13}$=3.0×10$^9$ M$^{-1}$s$^{-1}$ (S13)

At a given reaction time *t*, there is competitive kinetics between benzene and phenol:

$$\frac{d[benzene]_t}{dt} = -k_7[benzene]_t[SO_4^{\bullet-}]_{ss}$$

$$\frac{d[phenol]_t}{dt} = -k_{13}[phenol]_t[SO_4^{\bullet-}]_{ss}$$

Transform the above differential equation to numerical integration between reaction time $t_1$ and $t_2$:

$$\Delta[benzene]_{t_2-t_1} = -k_7 \frac{([benzene]_{t_1} + [benzene]_{t_2})}{2}[SO_4^{\bullet-}]_{ss,t_1\to t_2}(t_2 - t_1)$$

$$\Delta[phenol]_{t_2-t_1} = -k_{13} \frac{([phenol]_{t_1} + [phenol]_{t_2})}{2}[SO_4^{\bullet-}]_{ss,t_1\to t_2}(t_2 - t_1)$$

Therefore, $\Delta[phenol]_{t_2-t_1} = \frac{k_{13}}{k_7} \bullet \frac{[phenol]_{t_1} + [phenol]_{t_2}}{[benzene]_{t_1} + [benzene]_{t_2}}[SO_4^{\bullet-}]_{ss,t_1\to t_2}(t_2 - t_1)$

$\Delta[phenol]_{t_2-t_1}$ is the loss of phenol that should be accounted for as the oxidation product of benzene. Therefore, the total amount of phenol produced between the reaction time $t_1$ and $t2$ is:

$$\Delta[phenol]_{produced,t_2-t_1} = \Delta[phenol]_{measured,t_2-t_1} + \Delta[phenol]_{t_2-t_1}$$

Based on the calculation, $\Delta[\text{phenol}]_{t2\text{-}t1}$ is a very small fraction, *i.e.*, $\Delta[\text{phenol}]_{t2\text{-}t1}$ is <0.1% of $\Delta[\text{phenol}]_{\text{measured, t2-t1}}$. Therefore, the loss of phenol due to reaction with $SO_4^{\cdot-}$ is negligible.

In addition, since $[HO^{\cdot}]_{ss}$ is 2 orders of magnitude smaller than $[SO_4^{\cdot-}]_{ss}$, and the rate constant of phenol reacting with $HO^{\cdot}$ ($k$=6.6×10$^9$ M$^{-1}$s$^{-1}$) is similar to that of phenol reacting with $SO_4^{\cdot-}$ ($k$=8.8×10$^9$ M$^{-1}$s$^{-1}$), the loss of phenol due to reaction with $HO^{\cdot}$ is negligible as well.

**Table S1** Characterization of aquifer materials, clay materials and pure minerals.[1]

| Material Type | Material Name | BET Surface area ($m^2/g$) | Total Fe (wt %) | Total Mn (wt %) | Sand (wt %) | Silt (wt %) | Clay (wt%) |
|---|---|---|---|---|---|---|---|
| **Aquifer Material** | CADOU | 3.9 | 0.77% | 0.01% | 84% | 16% | 4% |
| | CAROL | 39.8 | 2.49% | 0.02% | 63% | 18% | 19% |
| | AWBPH | 14.3 | 1.67% | 0.03% | 82% | 10% | 8% |
| | AFTCS | 27.7 | 1.44% | 0.03% | 60% | 22% | 18% |
| | AMTAL | 16.2 | 1.85% | 0.12% | 64% | 22% | 14% |
| **Clay Material** | Nontronite | 69.0 | 26.2% | 0.01% | -- | -- | 100% |
| | Montmorillonite | 32.0 | 2.6% | 0.05% | -- | -- | 100% |
| **Pure Mineral** | Geothite $\alpha$-$FeOOH_{(s)}$ | 37.1 | 62.9% | -- | -- | -- | -- |
| | Ferrihydrite $Fe(OH)_{3(s)}$ | 180.1 | 52.3% | -- | -- | -- | -- |
| | Pyrolusite $\beta$-$MnO_{2(s)}$ | 0.11 | -- | 62.8% | -- | -- | -- |
| | Silica $SiO_{2(s)}$ | 27.0 | -- | -- | -- | -- | -- |

**Table S2** Chemical composition of synthetic groundwater used in this study.

| **Chemical parameter** | **Concentration** |
|---|---|
| $Na^+$ | 23 mg/L |
| $Ca^{2+}$ | 20 mg/L |
| $Mg^{2+}$ | 5 mg/L |
| $SO_4^{2-}$ | 20 mg/L |
| $Cl^-$ | 35.5 mg/L |
| $Br^-$ | 0.1 mg/L |
| $NO_3^-$ | 1 mg/L |
| $HCO_3^-$ | 1 mM |
| TDS | 166 mg/L |
| Suwannee River NOM | 1 mg C/L |
| pH | 8 |

The solution was buffered at pH 8.0 with 50 mM borate. The use of high buffer concentration was necessary to maintain a constant pH throughout the experiment.

- Experimental condition is with 50 g/L of minerals, initial persulfate concentration 1 mM and pH 8. In experiments with benzene, the initial concentration of benzene was 1 mM.

**Table S3** Comparison of the production of aldehyde-like compound relative to phenol by $S_2O_8^{2-}$ and $H_2O_2$.

| | **Relative ratio of aldehyde-like compound to phenol ($10^4$ AU/μM) *** | |
|---|---|---|
| | **$S_2O_8^{2-}$ activation** | **$H_2O_2$ activation** |
| **Goethite** | 0.33 ± 0.11 | 0.23 ± 0.01 |
| **Ferrihydrite** | 6.2 ± 2.4 | Aldehyde not detected |
| **Pyrolousite** | 0.26 ± 0.09 | Aldehyde not detected |

* The concentration of aldehyde-like compound is expressed as $\times 10^4$ adsorption units (AU) at the wavelength of 360 nm. The concentration of phenol is express as μM.

**Table S4** Comparison of oxidant yield in synthetic groundwater and MQ water from persulfate activation by different minerals*.

| | Yield of $SO_4^{\bullet-}$ from $S_2O_8^{2-}$ | Yield of $SO_4^{\bullet-}$ from $S_2O_8^{2-}$ |
|---|---|---|
| | **Synthetic Groundwater** | **MQ water** |
| **Goethite** | 155% ± 6% | 167% ± 10% |
| **Ferrihydrite** | 20% ± 10% | 26% ± 8% |
| **Pyrolousite** | 37% ± 5% | 62% ± 12% |

* Experimental condition: initial benzene=1 mM; initial persulfate=1 mM; mineral solids=50 g/L; pH=8.0; ionic strength=50 mM.

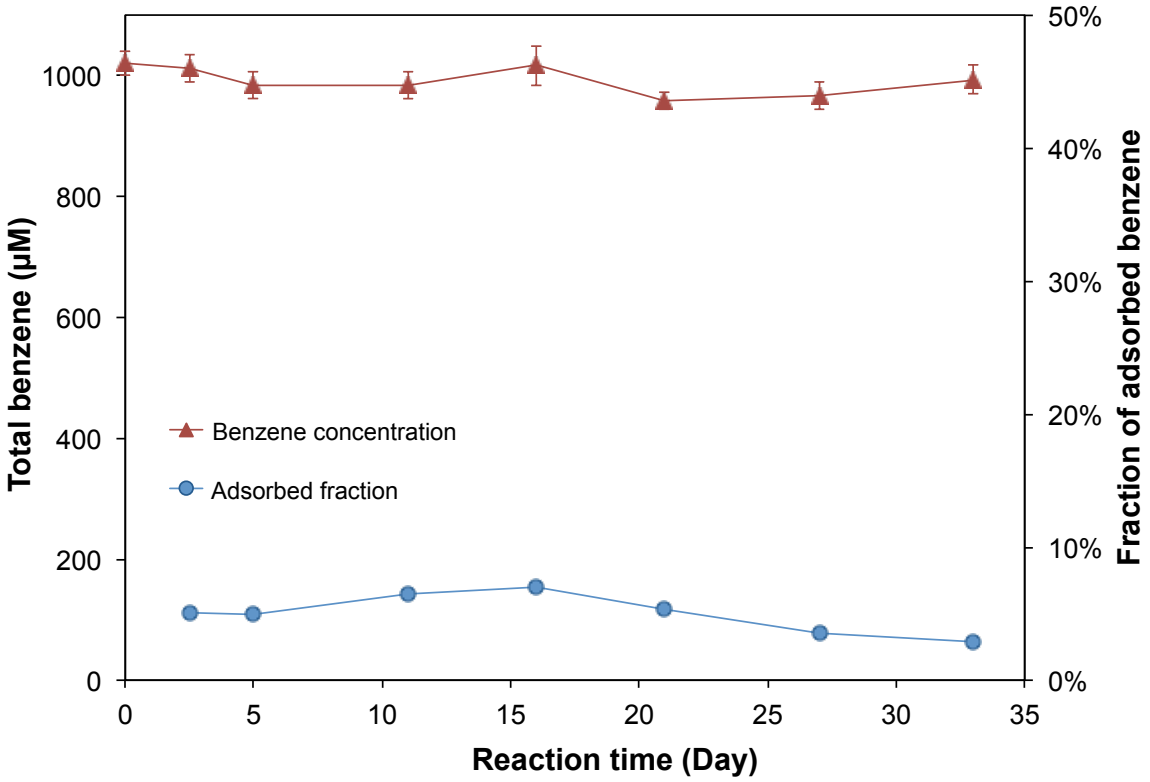


**Figure S1** Measurement of total benzene (*i.e.*, aqueous benzene plus adsorbed benzene) in a 50 g/L pyrolusite suspension. Adsorbed benzene was recovered by acetonitrile extraction. Initial added benzene was 1000 μM, pyrolusite concentration was 50 g/L, pH was buffered at 8.0 with 50 mM borate.

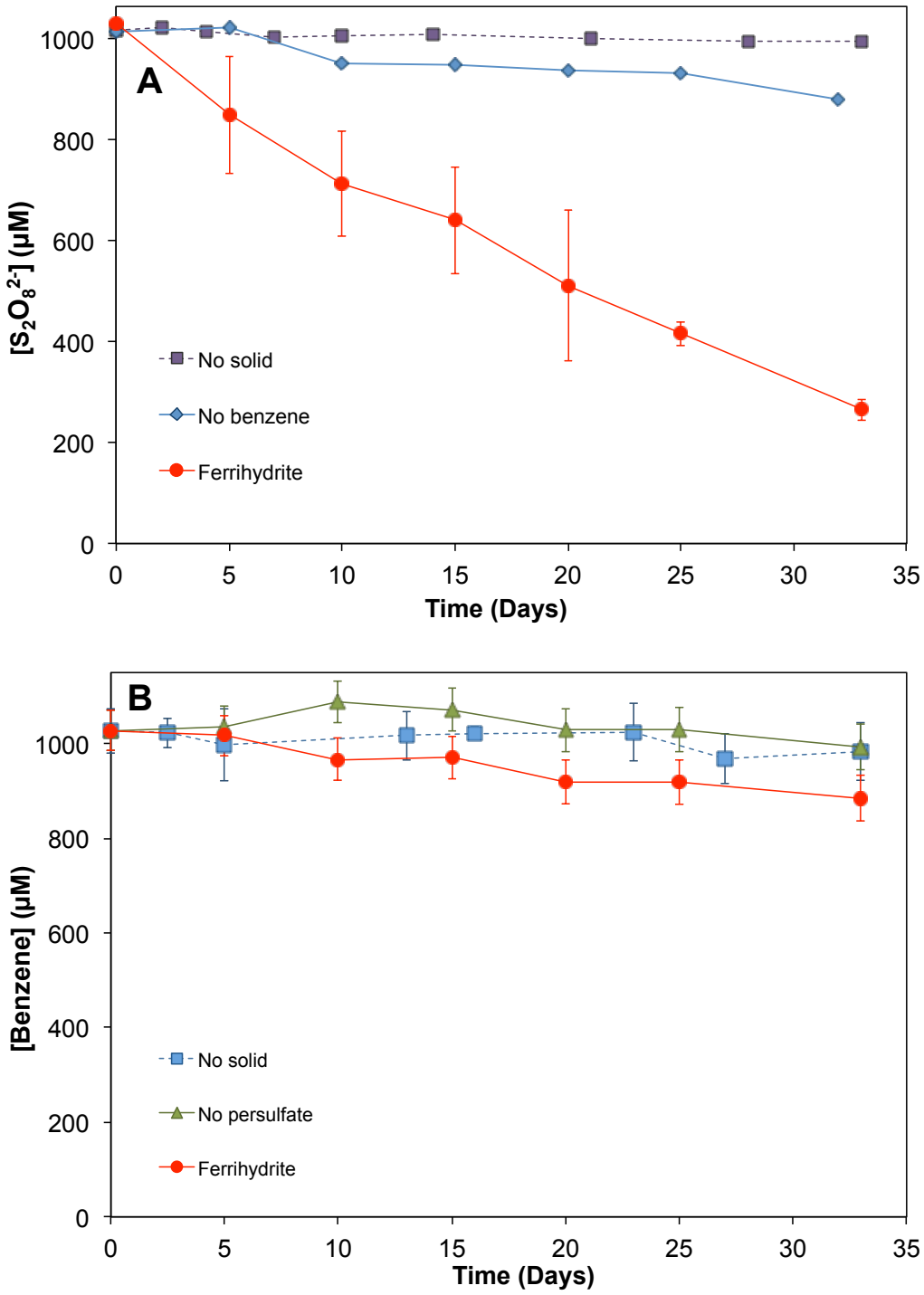


**Figure S2** Changes in (A) persulfate concentration and (B) total benzene concentration via persulfate activation in the presence of ferrihydrite ($Fe(OH)_{3(s)}$). Initial benzene=1 mM, initial persulfate=1 mM, ferrihydrite concentration=50 g/L, pH=8.0.

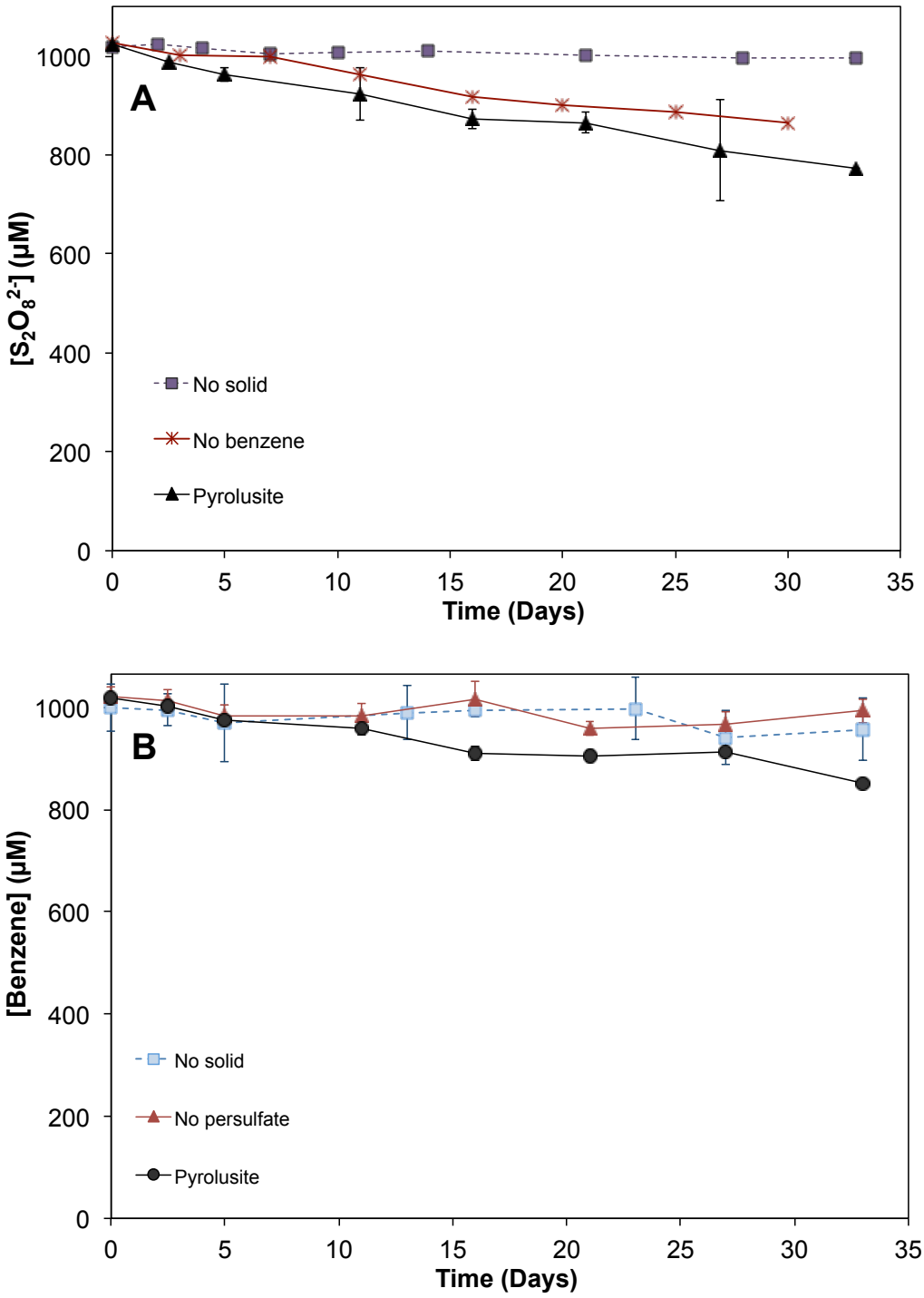


**Figure S3** Changes of (A) persulfate concentration and (B) total benzene concentration via persulfate activation in the presence of pyrolusite (β-$MnO_{2(s)}$). Initial benzene=1 mM, initial persulfate=1 mM, pyrolusite concentration=50 g/L, pH=8.0.

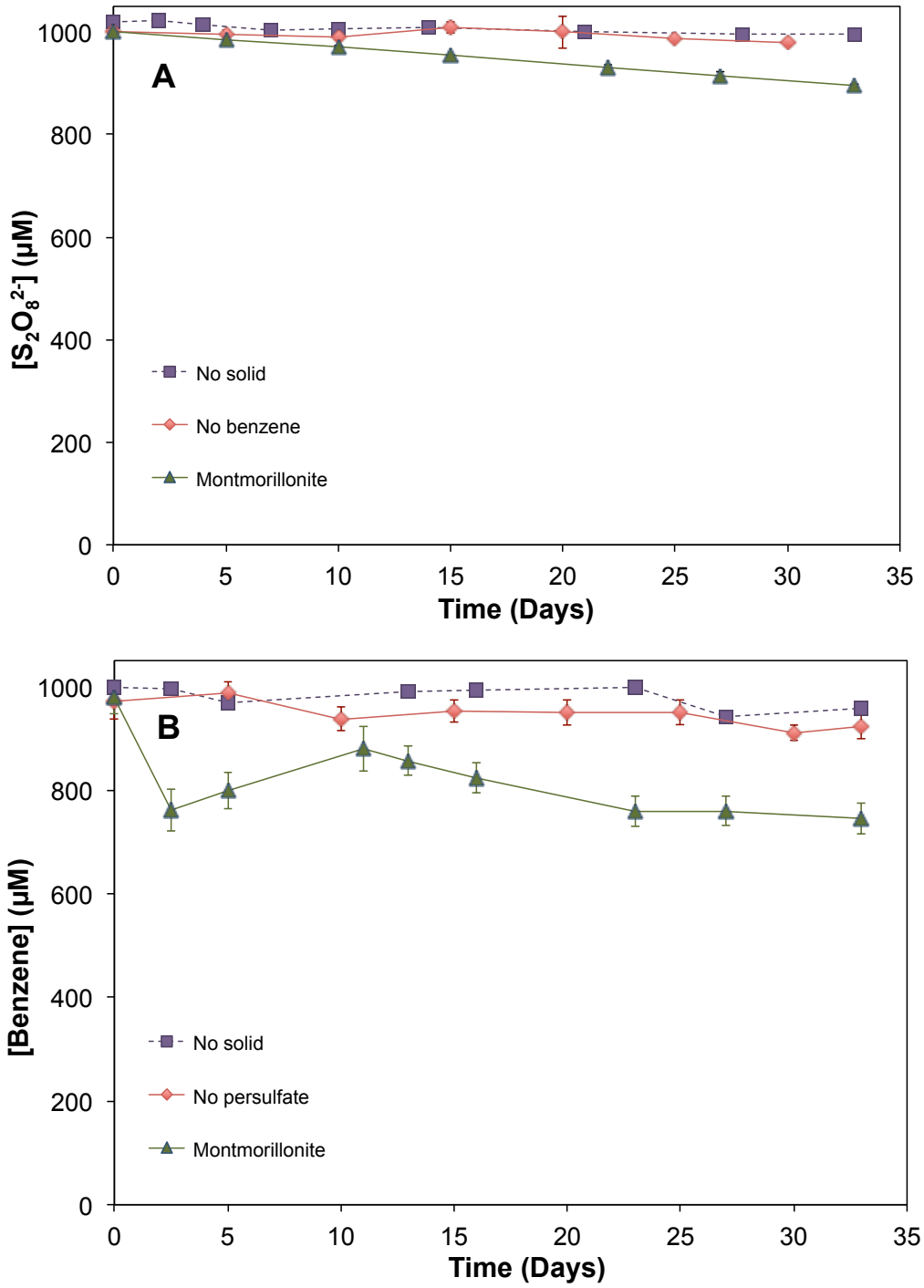


**Figure S4** Changes of (A) persulfate concentration and (B) total benzene concentration via persulfate activation in the presence of montmorillonite. Initial benzene=1 mM, initial persulfate= 1 mM, montmorillonite concentration=50 g/L, pH=8.0.

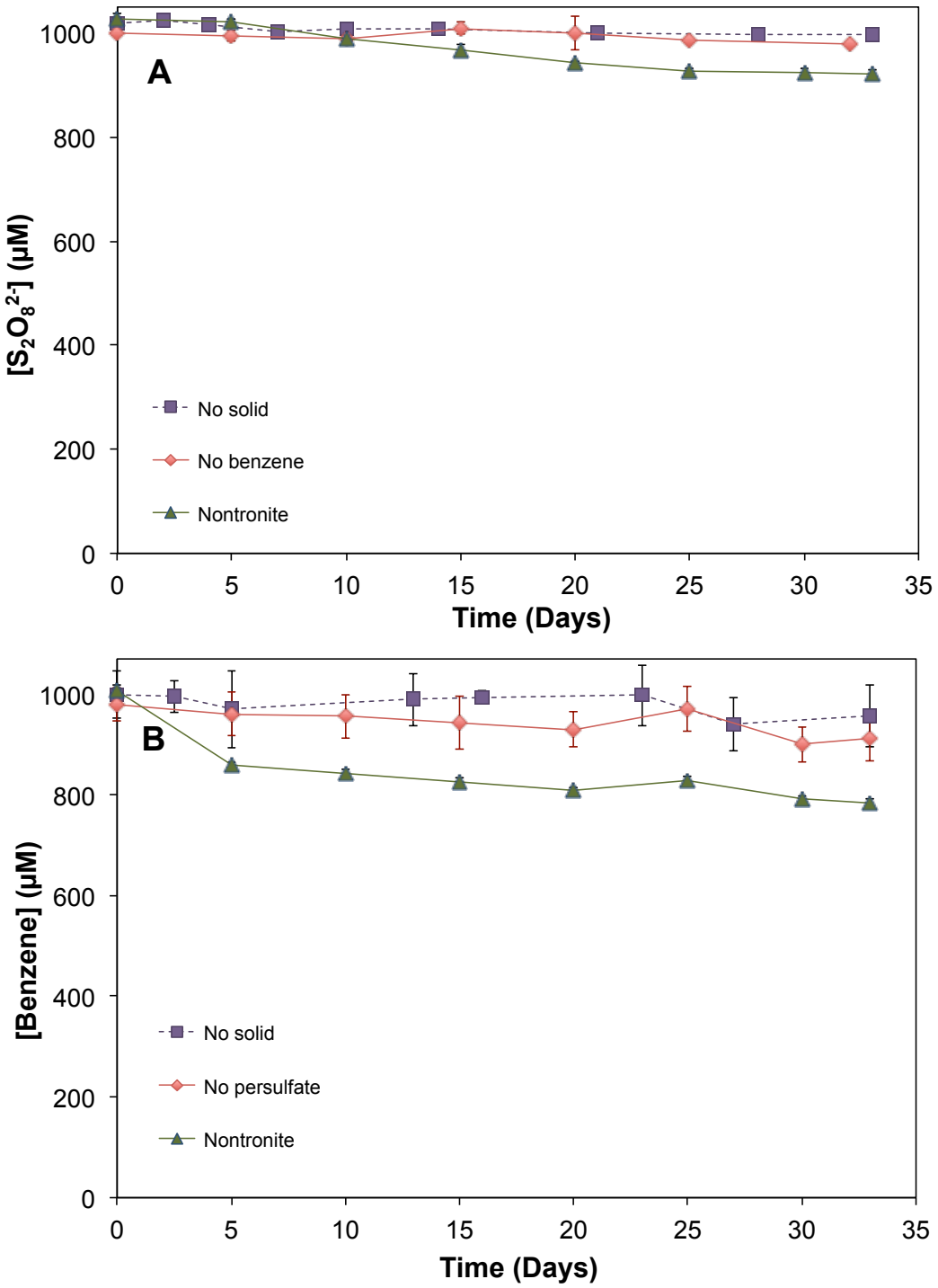


**Figure S5** Changes of (A) persulfate concentration and (B) total benzene concentration via persulfate activation in the presence of nontronite. Initial benzene=1 mM, initial persulfate 1 mM, nontronite concentration 50 g/L, pH 8.0.

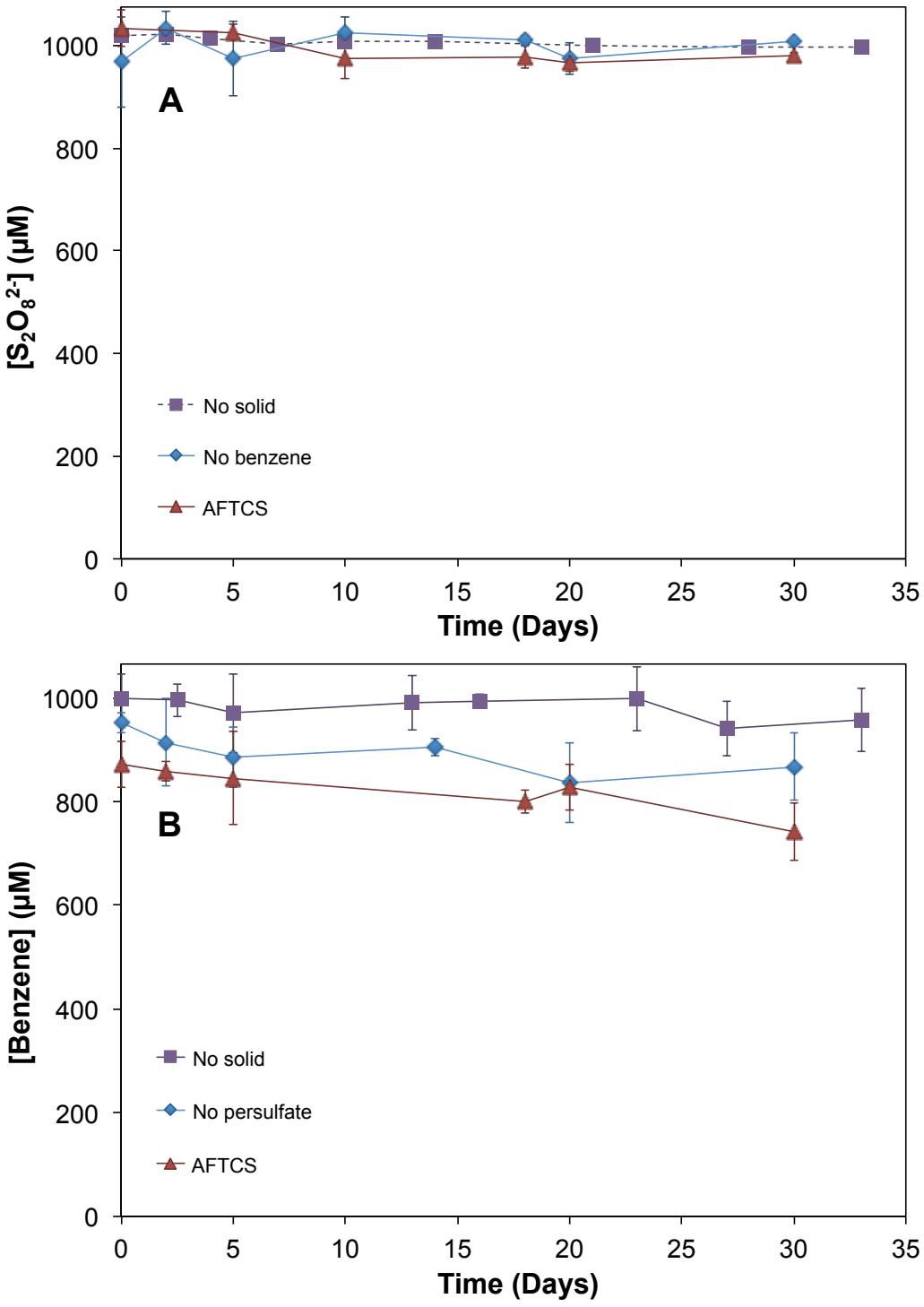


**Figure S6** Changes of (A) persulfate concentration and (B) total benzene concentration via persulfate activation in the presence of aquifer material AFTCS. Initial benzene=1 mM, initial persulfate=1 mM, AFTCS concentration=50 g/L, pH=8.0.

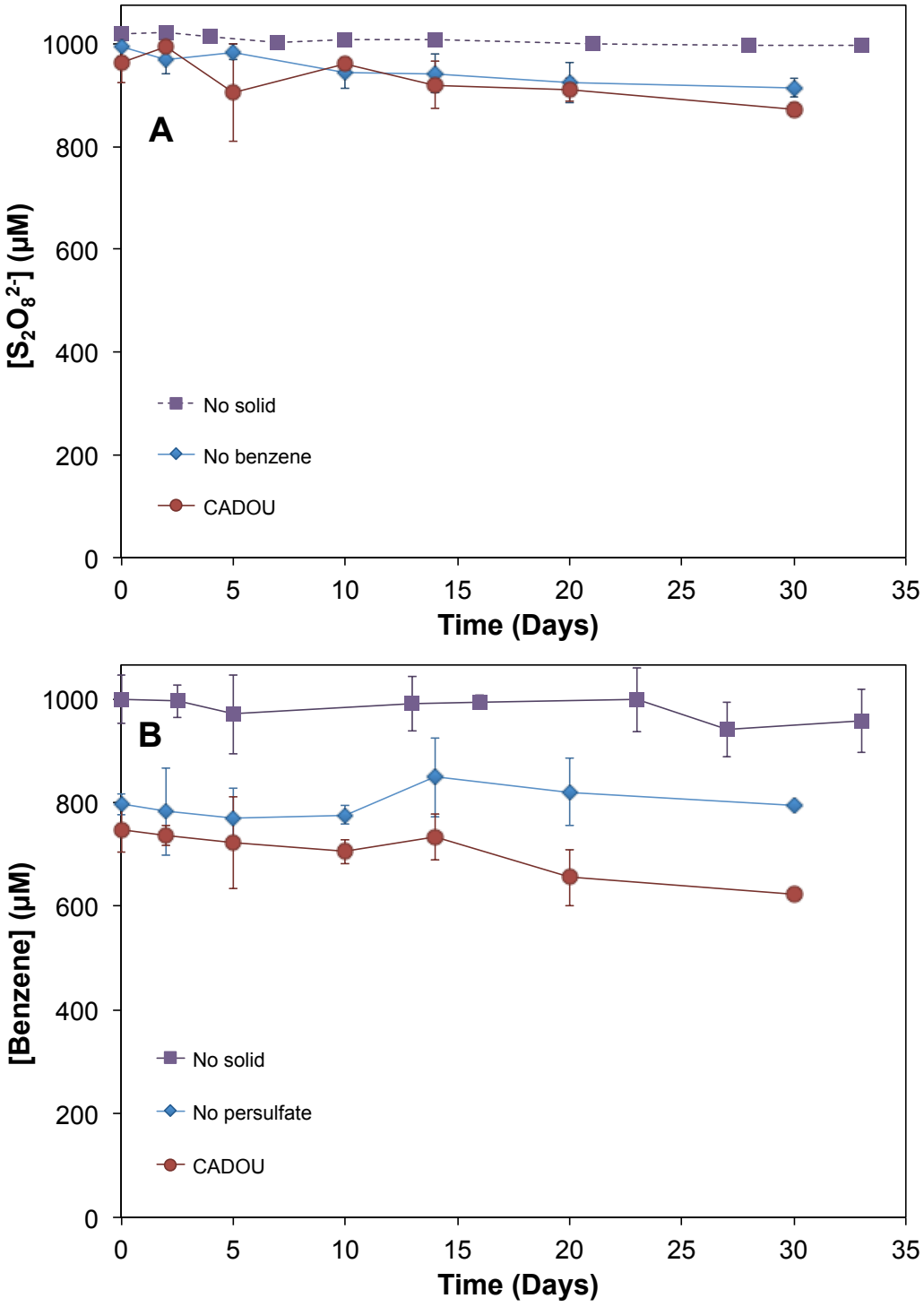


**Figure S7** Changes of (A) persulfate concentration and (B) total benzene concentration via persulfate activation in the presence of aquifer material CADOU. Initial benzene=1 mM, initial persulfate=1 mM, CADOU concentration=50 g/L, pH=8.0.

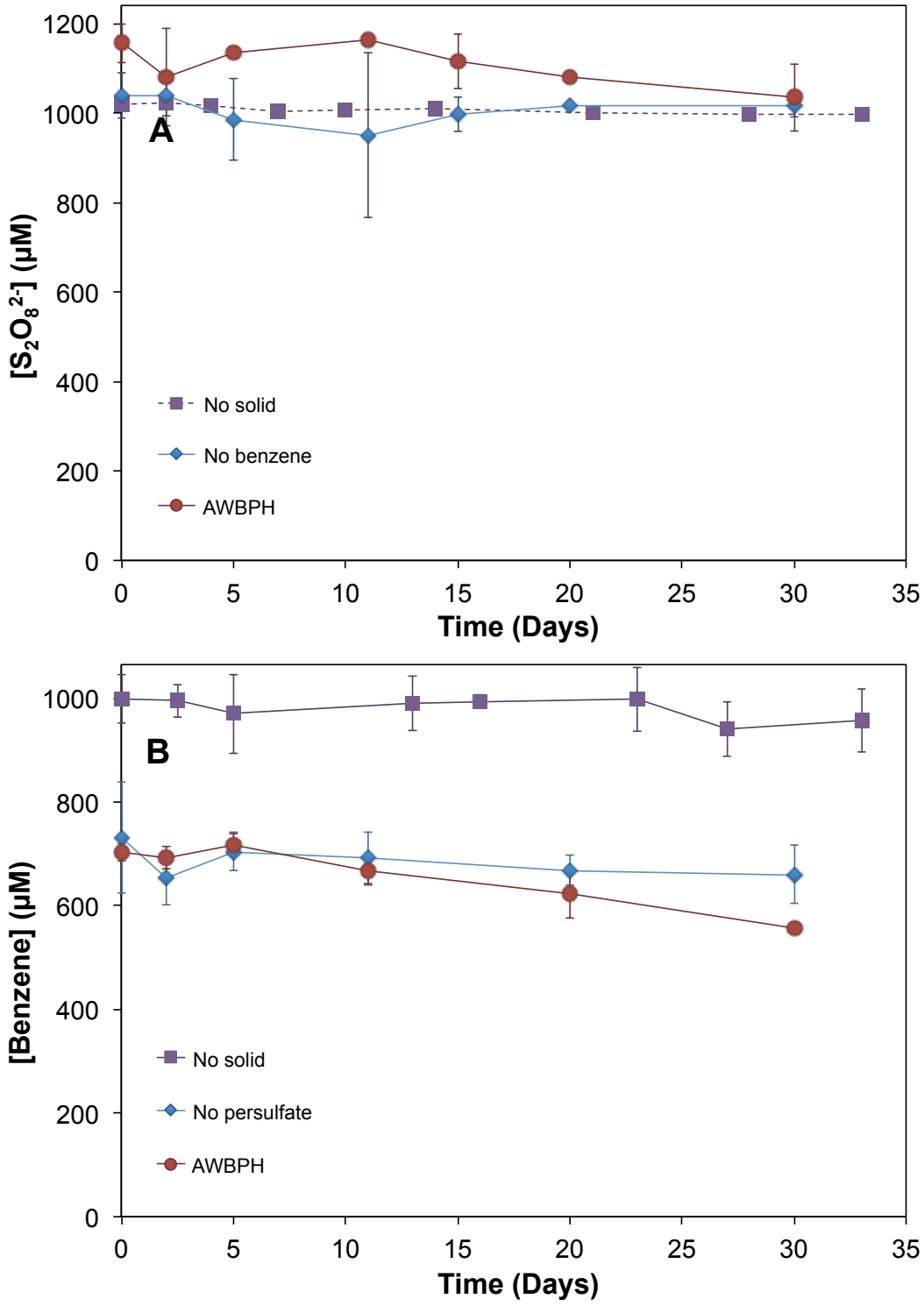


**Figure S8** Changes of (A) persulfate concentration and (B) total benzene concentration via persulfate activation in the presence of aquifer material AWBPH. Initial benzene=1 mM, initial persulfate=1 mM, AWBPH concentration=50 g/L, pH=8.0.

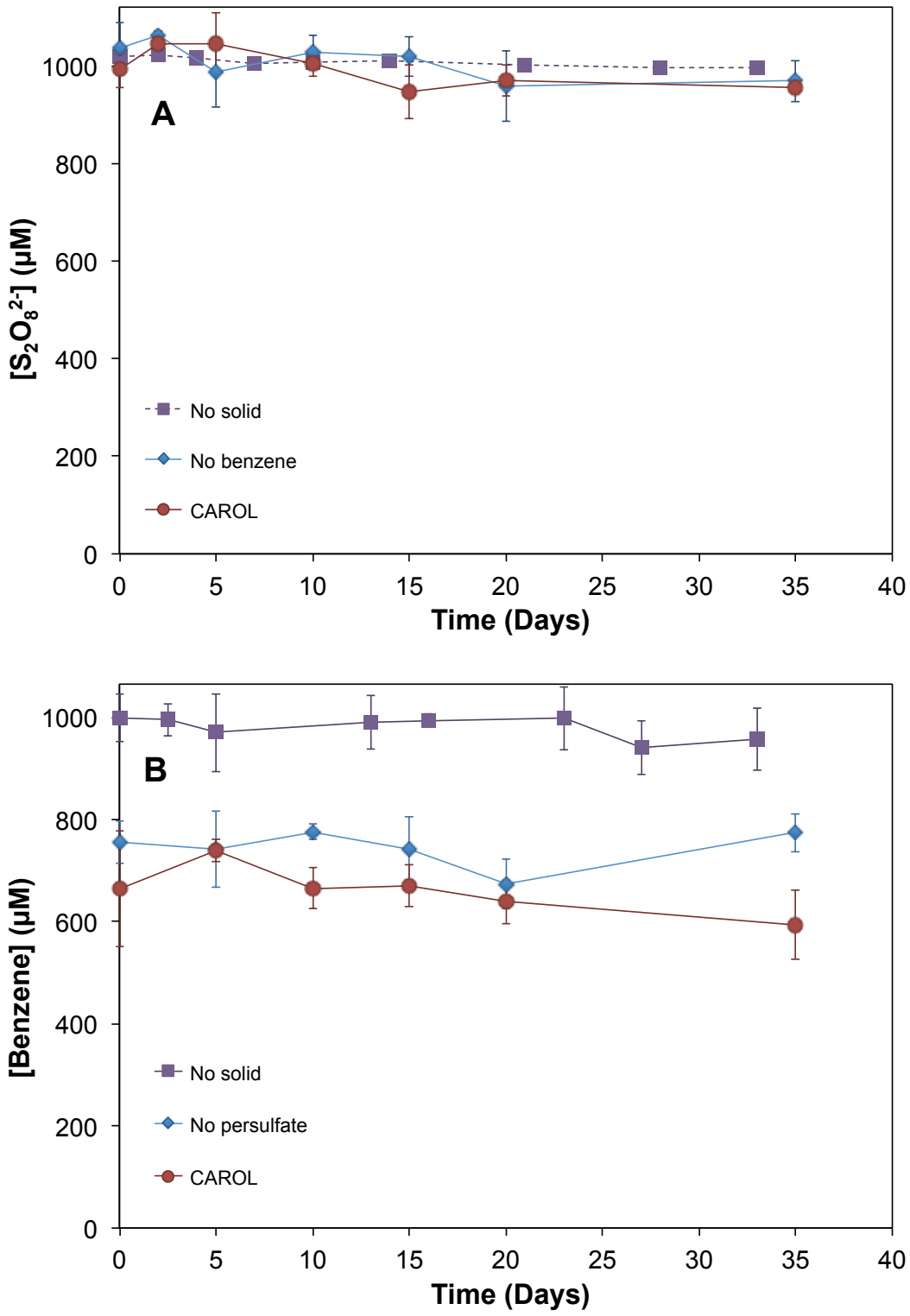


**Figure S9** Changes of (A) persulfate concentration and (B) total benzene concentration via persulfate activation in the presence of aquifer material CAROL. Initial benzene=1 mM, initial persulfate=1 mM, CAROL concentration=50 g/L, pH=8.0.

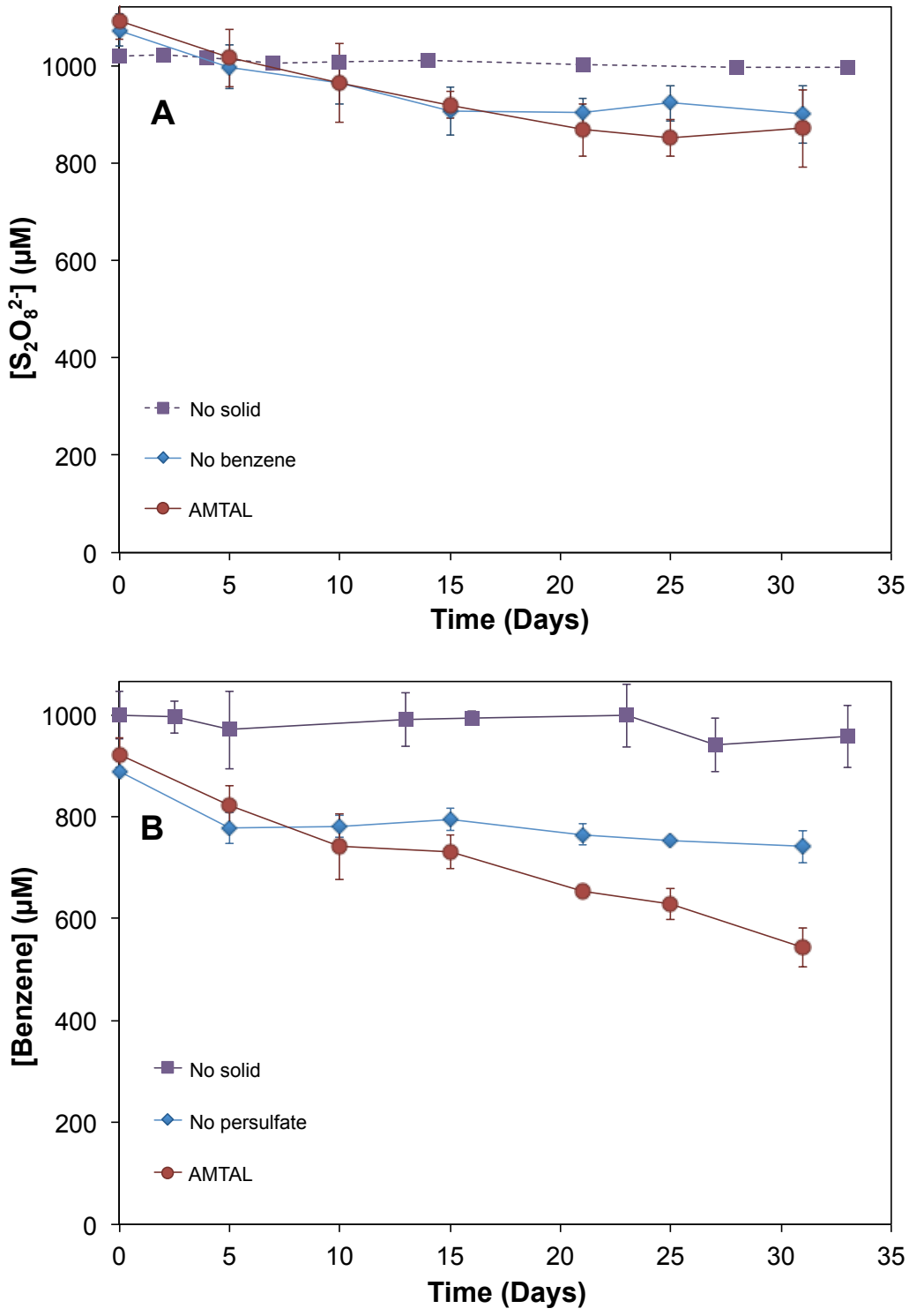


**Figure S10** Changes of (A) persulfate concentration and (B) total benzene concentration via persulfate activation in the presence of aquifer material AMTAL. Initial benzene=1 mM, initial persulfate=1 mM, AMTAL concentration=50 g/L, pH=8.0.

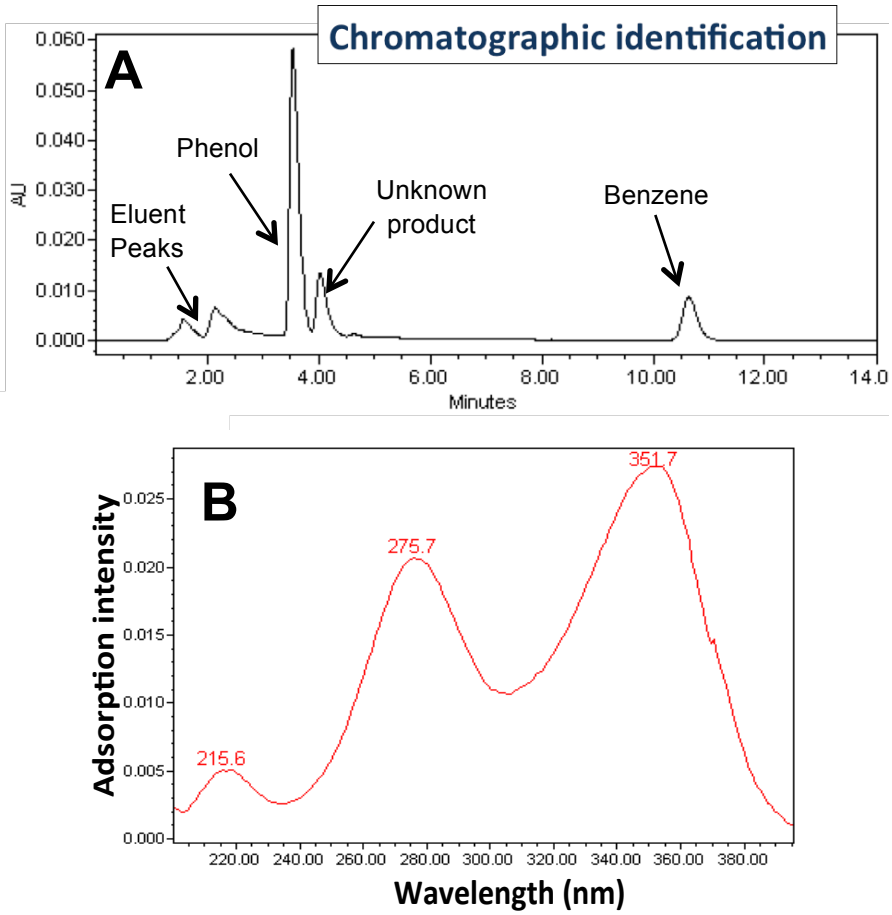
Chromatographic identification
A
Phenol
Eluent
Peaks
Unknown
product
Benzene
AU
0.060
0.050
0.040
0.030
0.020
0.010
0.000
2.00
4.00
6.00
8.00
10.00
12.00
14.0
Minutes
B
351.7
275.7
215.6
Adsorption intensity
0.025
0.020
0.015
0.010
0.005
0.000
220.00
240.00
260.00
280.00
300.00
320.00
340.00
360.00
380.00
Wavelength (nm)

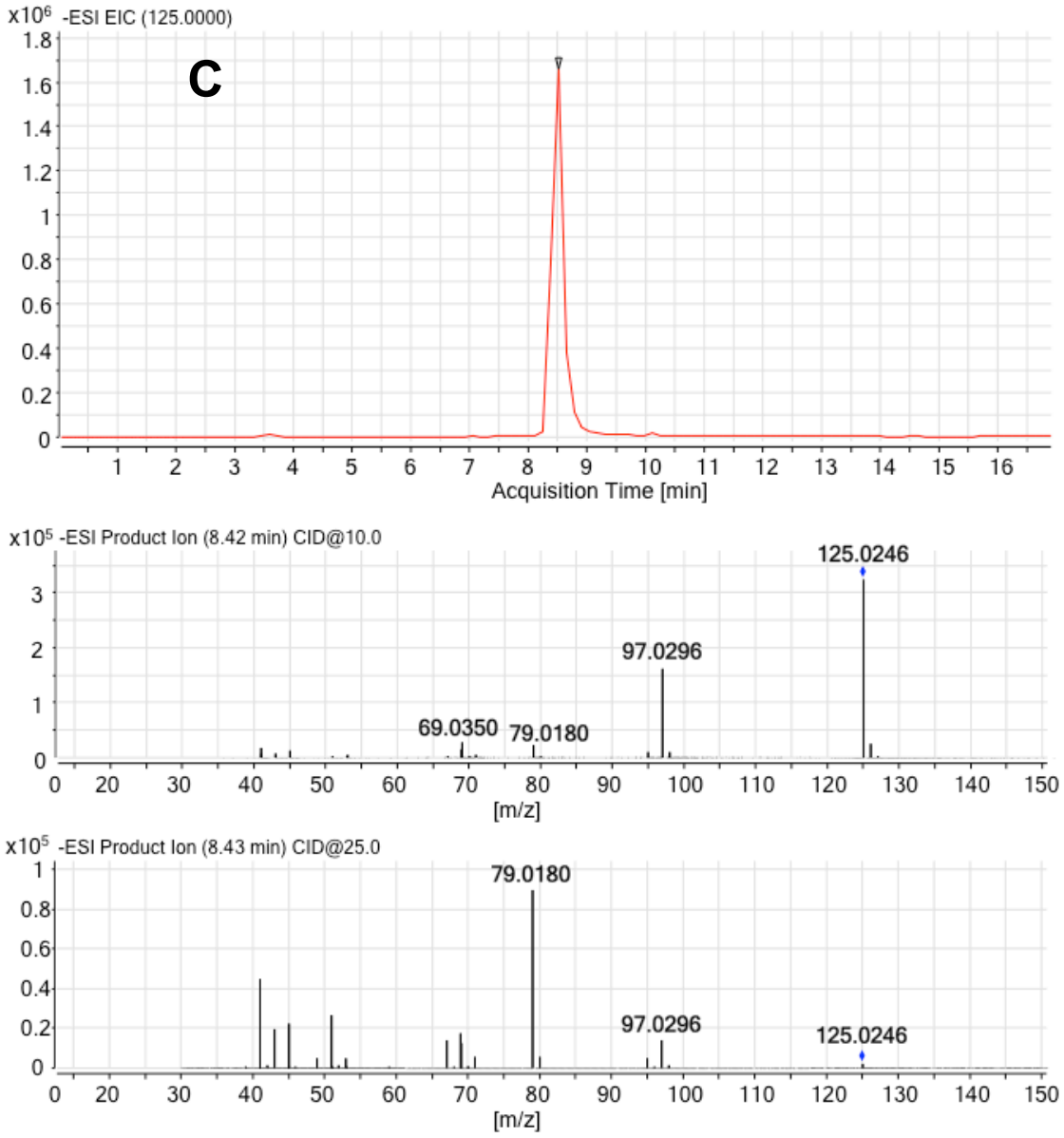


**Figure S11** Identification of aldehyde-like compound as the oxidation product of benzene by $SO_4^{\bullet-}$ radicals. (A) HPLC-UV chromatogram of one sample obtained after persulfate was activated in the presence of benzene and minerals; (B) UV Spectra of the aldehyde-like product; (C) QTOF-LC-MS scan in negative mode of the aldehyde-like product. An exact mass of m/z 125.0246 was obtained, which corresponds to the sum formula $C_6H_5O_3$ (Δppm: 5.6).Fragmentation of the m/z 125 revealed cleavage of CO (-28 Da; fragments 97.0296 and 69.0350). At higher collision energies fragment 79.0180 increased indicating the cleavage of $H_2O$ (-18 Da) from fragment 97.0296.

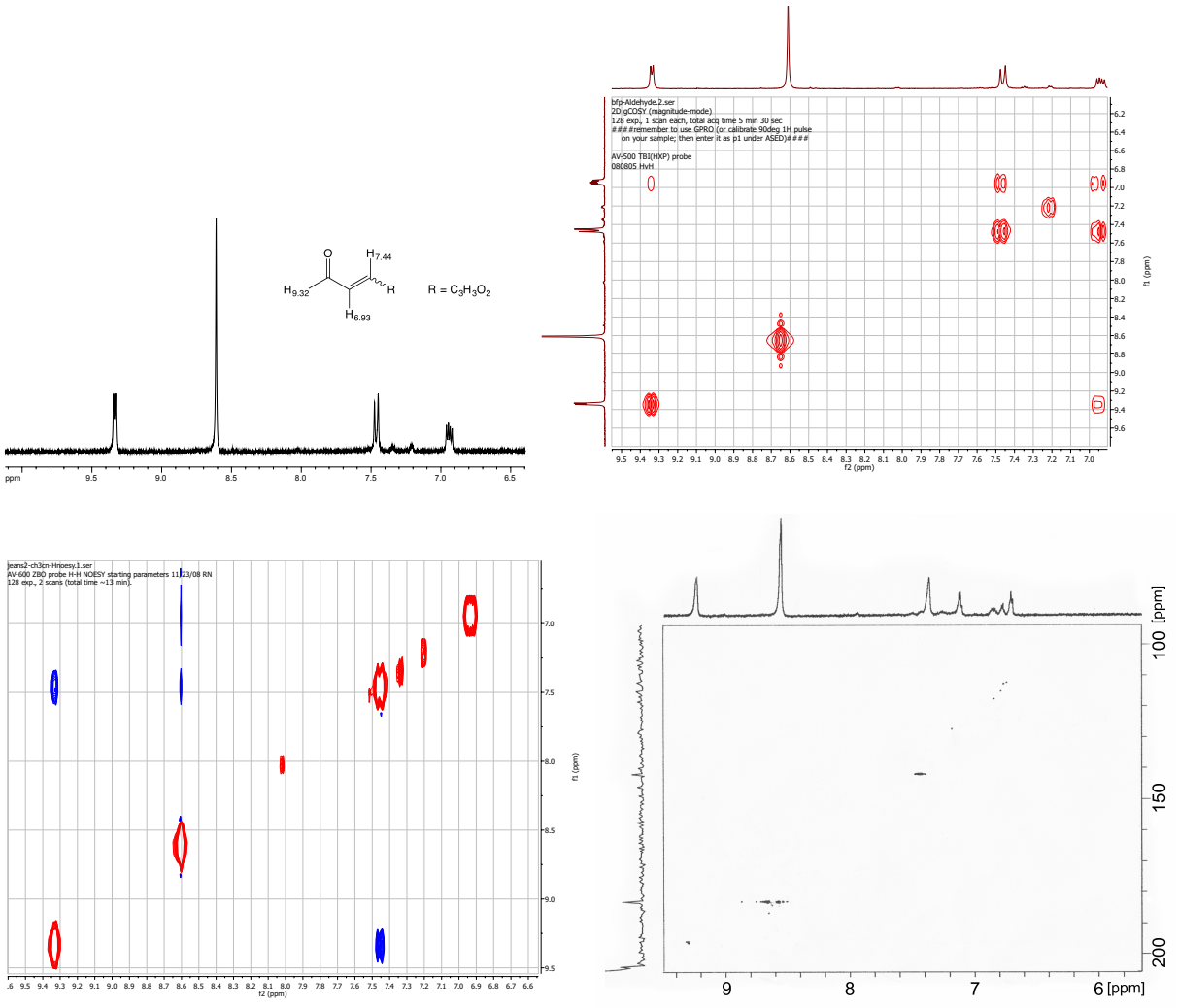


**Figure S12** NMR spectra of the unknown compound confirm a ring cleavage product with a fragment identified as an enal. $^{1}$H NMR (top left), $^{1}$H,$^{1}$H-NOESY (top right), $^{1}$H,$^{1}$H-COSY (bottom left), $^{1}$H,$^{13}$C-HSQC (bottom right). $^{1}$H NMR (600 MHz, $CD_3CN$) δ 9.32 (d, 1 H, $J$ = 10), 8.63 (s, 2 H), 7.44 (d, 1 H, $J$ = 15), 6.93 (dd, 1 H, $J$ = 10, 15). $^{1}$H-$^{13}$C HSQC (600 MHz, 151 MHz, $CD_3CN$) δ (9.32, 198.5), (8.63, 185), (7.44, 143), (6.93, 115). MestReNova and iNMR (Mestrelab Research SL) were used to process the NMR spectra. Chemical shifts are reported in ppm and calibrated to residual solvent peaks. Coupling constants are reported in hertz. Unidentified peaks in the HSQC are due to contamination with phenol.

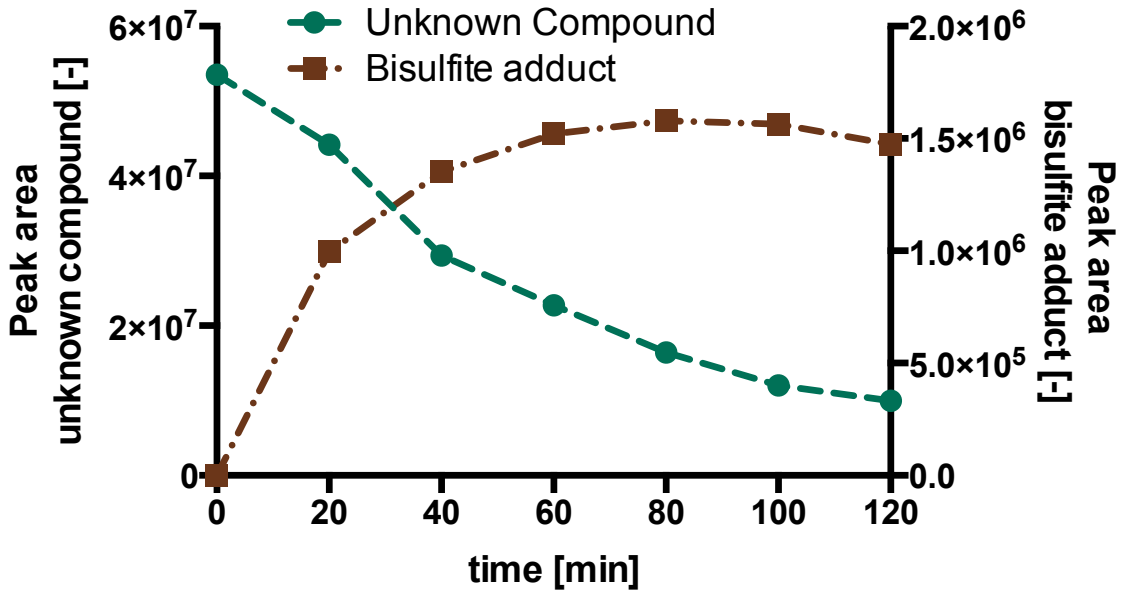


**Figure S13** Formation of a bisulfite adduct of the unknown ring-cleavage product over time. The increase of the peak area for the bisulfite-adduct product indicated the presence of an aldehyde moiety. 10 mM bisulfite was mixed with SPE-enriched ring-cleavage product.

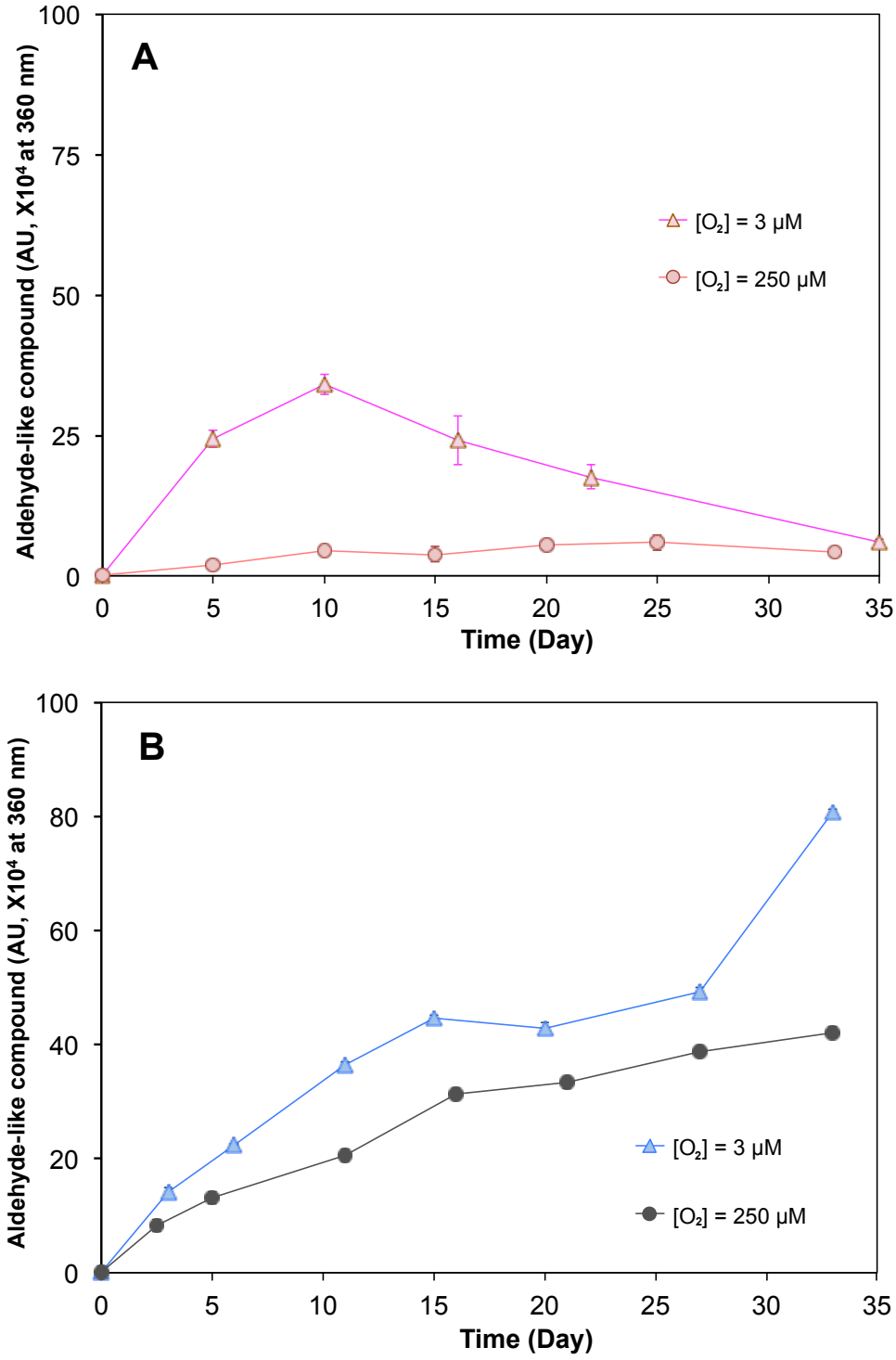


**Figure S14** Formation of aldehyde-like product during persulfate activation by minerals. (A) Ferrihydrite; (B) Pyrolusite. Mineral mass loading=50 g/L, initial total benzene=1000 μM, initial $S_2O_8^{2-}$=1000 μM, borate buffer=50 mM, pH=8.0.

**References**


1 Liu, H.; Bruton, T. A.; Doyle, F. M.; Sedlak, D. L. In situ chemical oxidation of contaminated groundwater by persulfate: activation by Fe(III)- and Mn(IV)-containing oxides and aquifer materials. *Environ. Sci. Technol.* **2014**, 48, 10330-10336.

2 Anipsitakis, G. P.; Dionysiou, D. D. Degradation of organic contaminants in water with sulfate radicals generated by the conjunction of peroxymonosulfate with cobalt. *Environ. Sci. Technol.* **2003**, *37* (20), 4790-4797.

3 Zhang, T.; Zhu, H.; Croué, J. P. Production of sulfate radical from peroxymonosulfate induced by a magnetically separable $CuFe_2O_4$ spinel in water: efficiency, stability and mechanism. *Environ. Sci. Technol.* **2013**, *47* (6), 2784-2791.

4 Zhang, Z.; Edwards, J. O. Chain lengths in the decomposition of peroxomonosulfate catalyzed by cobalt and vanadium. Rate law for catalysis by vanadium. *Inorg. Chem.* **1992**, *31* (17), 3514-3517.

5 Kolthoff, I. M.; Miller, I. K. The chemistry of persulfate. I. The kinetics and mechanism of the decomposition of the persulfate ion in aqueous medium. *J. Am. Chem. Soc*. **1951**, *73* (7), 3055-3059.

6 Herrmann, H.; Reese, A.; Zellner, R. Time-resolved UV/VIS diode-array absorption spectroscopy of $SO_x^-$ (x=3, 4, 5) radical anions in aqueous solution. *J. Mol. Struct.* **1995**, *348*, 183-186.

7 Peyton, G. R. The free-radical chemistry of persulfate-based total organic carbon analyzer. *Mar. Chem.* **1993**, *41*, 91-103.

8 Buxton, G. V.; Greenstock, C. L.; Helman, W. P.; Ross, A. B. Critical review of rate constants for reactions of hydrated electrons, hydrogen atoms and hydroxyl radicals ($^{\bullet}OH/^{\bullet}O^-$) in aqueous solution. *J. Phys. Chem. Ref. Data.* **1988**, *17*, 513-886.

9 Das, T. N. Reactivity and role of $SO_5^{\bullet-}$ radical in aqueous medium chain oxidation of sulfite to sulfate and atmospheric sulfuric acid generation. *J. Phys. Chem. A.* **2001**, *105*, 9142-9155.

10 Pan, X. M.; Schuchmann, M. N.; von Sonntag, C. Oxidation of benzene by the HO radical: a product and pulse radiolysis study in oxygenated aqueous solution. *J. Chem. Soc. Perkin Trans.* **1993**, *2*, 289-297.